Bistable Charge-Transfer Complex Formation of Redox-Active Organic Molecules Based on Intermolecular HOMO−LUMO Interaction Controlled by the Redox Reactions

Bunji Uno,* Noriko Okumura, and Kunimasa Seto

Gifu Pharmaceutical University, Mitahora-higashi, Gifu 502-8585, Japan

Received: December 6, 1999; In Final Form: January 31, 2000

Bistable complex formation systems consisting of biphenylene (BP) and redox-active organic molecules such as chloranil (CL) and TCNE have been experimentally and theoretically investigated, based on an intermolecular interaction which characteristically occurs in the electrogenerated dianions forming a $\pi-\pi$ type charge-transfer (CT) complex. Initially, we examined the CT complex formation of CL^{2-} and $TCNE^{2-}$ with hydrocarbons (BP, hexamethylbenzene (HMB), and anthracene (AN)). Spectroelectrochemistry evidently gave the intermolecular CT spectra in the $CL^{2-}-BP$ and $TCNE^{2-}-BP$ systems at 500 and 550 nm, respectively. The CT interaction between the dianions and BP was measured as the positive shift of the second reduction potential with increasing concentrations of BP. This behavior allowed the formation constants to be estimated as 33.9 and 20.3 dm^3 mol^{-1} at 25 °C for the CL^{2-} and $TCNE^{2-}$ complexes in CH_2Cl_2 containing 0.5 mol dm^{-3} tetrabutylammonium perchlorate, respectively. Temperature dependence of the formation constants yielded the formation energy as 31.6 and 39.8 kJ mol^{-1} for the $CL^{2-}-BP$ and $TCNE^{2-}-BP$ systems, respectively. However, the CT spectra and the marked behavior in the voltammograms were not observed in the dianion systems involving HMB and AN. The $RHF/6-31G(d)$ calculations reveal that the $CL^{2-}-BP$ and $TCNE^{2-}-BP$ complex formations are due to molecular recognition based on the favorable intermolecular HOMO−LUMO interaction of the dianions with BP, and the geometries of the dianion complexes differ from those of the neutral complexes. This background led to the development of redox-mediated bistable complex formation systems characterized by the geometrical alteration and the chromatic change. The interconversion of the bistable complex formation in the systems is modulated through redox control of the intermolecular HOMO−LUMO interaction, with trichromic change arising from the neutral complex formation, the anion radical generation, and the dianion complex formation.

Introduction

Molecular recognition is well recognized to play crucial roles in molecular redox switches and shuttles involving bistable molecular or supramolecular species presenting two forms, whose interconversion can be modulated by redox reactions, as well as in various molecular switch systems.[1−3] Active investigations on the redox-mediated molecular recognition of organic molecules have provided extensive information concerning the intricate and efficient interdependence between molecular recognition and redox events in biological systems.[2,3] The effect of the various molecular recognition elements on the redox behavior and physical properties of redox-active organic molecules has been probed by Rotello's and Kaifer's groups and others.[2−7] The conformational and physical properties in such molecular recognition systems result in differences in metal coordinate,[4] hydrophobic,[2,5] hydrogen bonding and aromatic π-stacking interactions[3,6] in the redox states of the components. Considerable interest has been paid to the organic dianions as well as dications[2] that contribute to such molecular-level recognition elements as a part of the redox species, exhibiting specific recognition arising from strong electron donation due to their peculiar electronic states. We are particularly interested in the $\pi-\pi$ charge-transfer (CT) interaction of the organic π-dianions, as it is a novel phenomenon caused by the peculiar π-electronic system significantly affected by the two-electron addition to the antibonding LUMO.

Investigations on the π-dianions are, however, limited in terms of aromaticity and electronic multiplicity,[7,8] structural and spectral properties,[8−13] reactivity,[14] and the intermolecular interactions with cationic species and hydrogen donors,[9,10,15,16] whereas the characteristics of the anion radical are well documented. The most widely investigated dianions are quinones with regard to their biological functions and the coupled electron and proton transfer in the hydrogen-bonding systems.[9,10,15] In the area of organic molecular metamagnetism and ferromagnetism, considerable interest has been devoted to understanding of the structure−function relationship of metallocenium salts of strong acceptor anions such as the dianionic species of TCNE and TCNQ.[13] The chemistry of the organic π-dianions is being actively developed with a view to understanding the peculiar properties and the characteristic functions. Olah and co-workers have investigated the electronic states of dianions on the basis of Hückel's rule.[8] Their conclusions inspire research of dianions into characterization on molecular recognition of the dianions and the $\pi-\pi$ interaction with other π-electronic systems. There is, however, no report on the $\pi-\pi$ CT interaction of organic π-dianions and the design of the molecular devices based on the interaction.

In this paper the $\pi-\pi$ CT complex formation ability of the dianions of redox-active compounds such as chloranil (CL) and TCNE has been primarily studied by electrochemical and spectroelectrochemical methods. The measurements provide a unique probe into the molecular selectivity and geometries in the CT complex formation of the dianions. It is imperative to

Bistable Charge-Transfer Complex Formation

J. Phys. Chem. A, Vol. 104, No. 13, 2000 **3065**

perform an in-depth study of the fundamental principles for the CT complex formation of the dianions with the aid of molecular orbital (MO) calculations. This study would form the basis for the interpretation of future studies on highly designed redox-mediated molecular recognition systems utilizing the $\pi-\pi$ CT interaction of π-dianions.

Experimental Section

Chemicals. The chemicals used here were CL, TCNE, biphenylene (BP), anthracene (AN), and hexamethylbenzene (HMB), which were of the best available grade from Nacalai Tesque, Inc., Aldrich Chemical Co., and Acros Organics. CL and AN were recrystallized from acetone and methanol, respectively. TCNE was purified by repeated sublimation under reduced pressure. BP and HMB were used as received without further purification. All the samples were sufficiently dried under high vacuum prior to use. The solvent used for electrochemical and spectroelectrochemical measurements was CH_2Cl_2 of spectrograde purity commercially available from Nacalai Tesque, Inc., which was stored over molecular sieves (4A, Nacalai) for more than 2 days and then carefully rectified. Tetrabutylammonium perchlorate (TBAP) was used as a supporting electrolyte for CH_2Cl_2, being prepared by a dropwise addition of 70% perchloric acid to an aqueous tetrabutylammonium bromide solution, and being recrystallized three times from a mixture of ethyl acetate and pentane. TBAP was dried well under high vacuum just before use.

Electrochemical Measurements. Cyclic voltammetry was performed with a three-electrode system consisting of a glassy carbon working electrode, a coiled platinum counter electrode and a saturated calomel reference electrode (SCE). The voltammograms were run at a scan rate of 25 mV sec^{-1} using a BAS 100B electrochemical workstation, coupled to a FMV-5133D7 PC, and BAS electrochemical software to record and analyze the data. Temperature was maintained during the measurements by circulating constant-temperature ethanol throughout the cell compartment by the use of a Tokyo Rikakikai thermoleader, model UA-100. The sample solutions were prepared in a drybox completely filled with N_2 gas to prevent contamination by moisture. The solutions were purged with the N_2 gas to remove oxygen, and N_2 gas was passed over the solution during the measurements. Other details of the electrochemical measurements were described in a previous paper.[17]

Spectral Measurements. The CT spectra of the neutral CL and TCNE with hydrocarbons were recorded with a Shimadzu UV-240 spectrophotometer equipped with a cell holder temperature-controlled by circulating constant-temperature ethanol supplied from a Taiyo EZL-80 thermoleader. The details of the spectral measurements were described in previous papers.[18] Electronic spectra of TCNE$^-$ and TCNE^{2-} were observed with a Shimadzu SPD-M10A flow-type photodiode array detector with the optical path length of 1.0 cm, coupled to a Gateway P5$-$100 PC and Shimadzu M10A software to record and analyze the data.[9] The controlled-potential electrolyses were performed in a bulk electrolysis cell with a Hokuto Denko HA-501 potentiostat in a three-electrode mode consisting of a reticulated vitreous carbon working electrode, an Ag/AgNO$_3$ reference electrode (containing CH$_3$CN solution of 0.1 mol dm^{-3} TBAP and 0.01 mol dm^{-3} AgNO$_3$; BAS), and a coiled platinum wire counter electrode. The details of the spectroelectrochemical measurements were described in a previous paper.[9] In situ electrochemical ESR spectroscopy was performed with a JEOL JES$-$RE1X X-band spectrometer with 100 kHz magnetic field modulation. The controlled-potential electrolysis was performed
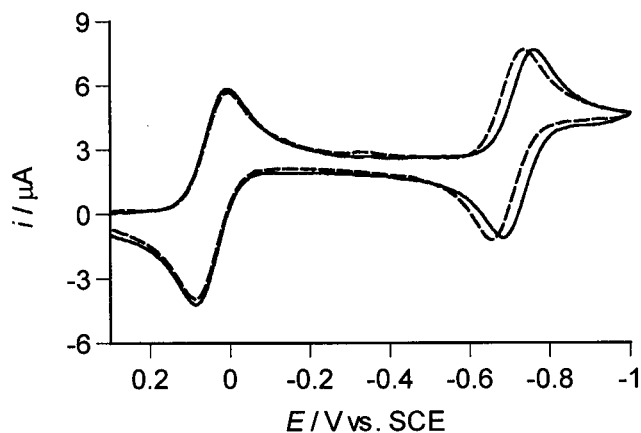

Figure 1. Cyclic voltammograms of 3.64×10^{-4} mol dm^{-3} CL in the absence ($-$) and the presence (- - -) of 9.65×10^{-3} mol dm^{-3} BP in the CH_2Cl_2 containing 0.1 mol dm^{-3} TBAP. Sweep rate = 25 mV s^{-1}.

at room temperature in an in situ electrochemical ESR cell using a 0.5-mm diameter straight platinum wire sealed in a glass capillary as a working electrode. Other details were described in a previous paper.[19]

MO Calculations. The geometries for the CL$-$BP, CL$^{2-}-$BP, TCNE$-$BP, and TCNE$^{2-}-$BP complexes were gradient optimized at the SCF level with the *Gaussian 98* program.[20] Postulating that CL^{2-} and TCNE^{2-} are closed-shell singlet species, the geometries were fully optimized in the RHF framework with 6-31G(d) basis sets (RHF/6-31G(d)) unless specified. The planar structures for the components of the complexes were kept in the geometry optimizations. Dependence of the complex formation upon the stacking angles (θ) of the components were examined by the RHF/6-31G(d) calculations for the orientation of various θ at every 10° angle. The complex formation energies were calculated by SCF and MP2 levels as the difference between the total energies of the CT complex and those of the free components. The post SCF calculations were done with the geometry optimized at the SCF level.

Results and Discussion

Electrochemistry and Spectroelectrochemistry of CL in the Presence of Hydrocarbons. Typical cyclic voltammograms of CL in the absence and the presence of BP are illustrated in Figure 1. In CH_2Cl_2, CL shows two cathodic polarographic waves, which correspond to the formation of the anion radical and the dianion, respectively, the energetics of these steps being discussed on the basis of MO calculations.[17] In these reductions, the first and second steps are reversible or at least quasi-reversible at customary scan rates, as shown in Figure 1. Addition of BP allowed the second half-wave reduction potential to be significantly shifted to the positive direction with no loss of reversibility, being indicative of substantial stabilization of CL^{2-}. The first wave on addition of BP is negligibly shifted to the negative direction.[21] Addition of the benzenoid hydrocarbons (AN, HMB) resulted in a shift of the first potential to less negative value without apparent affection to the second wave.[21] Thus, the positive shift of the second wave on addition of BP cannot be due to changes in bulk polarity, but must evidently be ascribed to quite specific CL$^{2-}-$BP interaction. This, of course, is not a particularly novel observation in electrochemistry. Certainly, the effect of stabilization of the reduced products on redox potentials has been recognized, particularly in the case of hydrogen bonds and cationic interaction of redox quinones and redox proteins.[10,15,22$-$24] These behaviors indicate that CL^{2-} selectively interacts only with BP among the hydrocarbons.
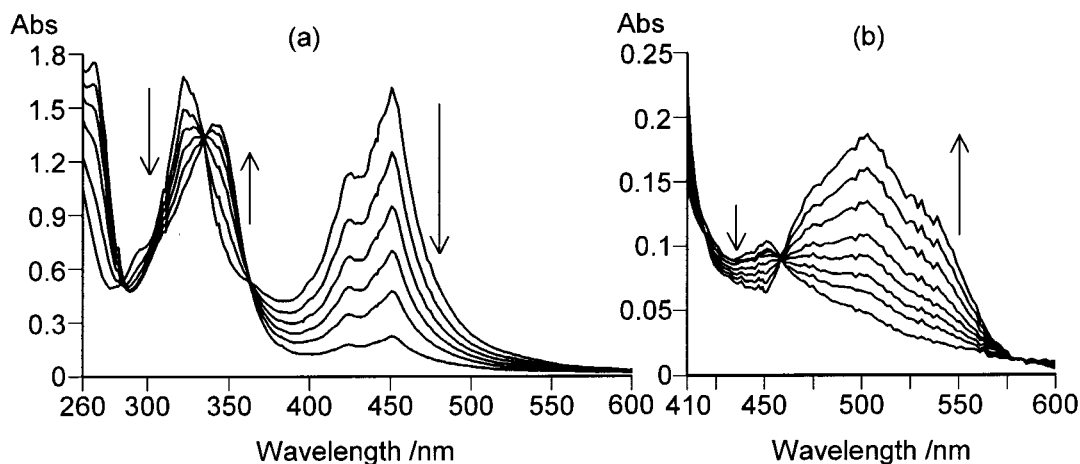
Figure 2. Spectral changes of CL in CH_2Cl_2 containing 0.5 mol dm^{-3} TBAP with controlled-potential electrolysis, corresponding to the CL^{2-} generation from CL$^-$ in the absence (a) and the presence (b) of 7.29×10^{-3} mol dm^{-3} BP. Concentrations of CL (mol dm^{-3}): (a) 2.59×10^{-4}, (b) 4.96×10^{-4}. Applied potential = -1.6 V vs Ag/AgNO$_3$.
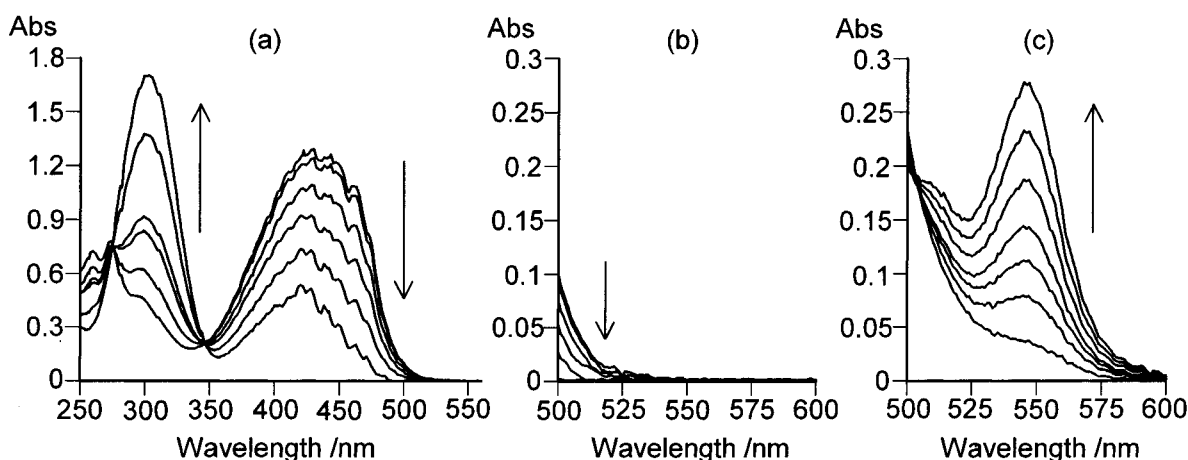

Figure 3. Spectral changes of TCNE in CH_2Cl_2 containing 0.5 mol dm^{-3} TBAP with controlled-potential electrolysis, corresponding to the TCNE^{2-} generation from TCNE$^-$ in the absence (a and b) and the presence (c) of 7.50×10^{-3} mol dm^{-3} BP. Concentrations of TCNE (mol dm^{-3}): (a and b) 2.76×10^{-4}, (c) 4.96×10^{-4}. Applied potential = -1.4 V vs Ag/AgNO$_3$.

To know what causes the positive shift of the second wave, the electronic spectra of the CL^{2-} were observed in the absence and the presence of BP. Spectroelectrochemistry of CL successfully gave the spectra of CL$^-$ and CL^{2-}, showing clear isosbestic points with electrolysis as a result of the reversible redox equilibria. Figure 2 shows the spectral changes with controlled-potential electrolysis of CL, corresponding to the CL^{2-} generation from CL$^-$. The spectral profile of CL^{2-} is the same as that previously observed for the 1,4-benzoquinone dianion.[9] By analogy with this analysis, the 340 nm band of CL^{2-} was assigned to the $^1B_{3u} \leftarrow \,^1A_g$ transition contributed mainly from the HOMO−LUMO electronic configuration under D_{2h} symmetry. In the presence of BP a new band appears at 500 nm with electrogeneration of CL^{2-}, resulting from CT interaction between CL^{2-} and BP, as shown in Figure 2b.[25] The solution apparently turns from yellow to red corresponding to the CL^{2-} generation from CL$^-$. On addition of HMB or AN, the spectral change in this wavelength region with electrolysis results only in decrease of the absorbance of CL$^-$ without observation of the 500 nm band. We therefore assign the positive shift of the second wave on addition of BP to changes in the fast CT complex formation equilibria which are closely coupled to reduction.

Electrochemistry and Spectroelectrochemistry of TCNE in the Presence of Hydrocarbons. Similarly, sequential electroreduction of TCNE in CH_2Cl_2 generated the corresponding anion radical and π-dianion, giving the two reversible waves ($+0.297$ and -0.716 V vs SCE) on the cyclic voltammogram. A qualitatively similar, continuous positive shift of the second wave of TCNE was observed on addition of BP. Addition of HMB also gave the same voltammetric behavior as that of CL. In the case of addition of AN we observed a decrease of the peak heights of both the first and second waves of TCNE and an irreversible multielectron reduction peak beginning near -1.4 V vs SCE. The green solution of the TCNE−AN complex prepared by a mix of the components promptly faded away. These phenomena may be ascribed to an inner complex formation via the π−π interaction between TCNE and AN.[26]

Spectroelectrochemistry of TCNE gave the spectra of TCNE$^-$ and TCNE^{2-} at 430 and 300 nm, respectively. Figure 3 shows the spectral change with the TCNE^{2-} generation from TCNE$^-$. The 300 nm band of TCNE^{2-} in CH_2Cl_2 is assigned to the $^1B_{3u} \leftarrow \,^1A_g$ transition of the planar D_{2h} structure.[27] Addition of BP to the TCNE solution allowed a new band resulting from the CT interaction between TCNE^{2-} and BP to appear at 550 nm with the electrogeneration of TCNE^{2-}, whereas in the absence of BP and in the presence of HMB or AN the spectral change in a wavelength region longer than 500 nm resulted only in decrease of the absorbance of TCNE$^-$, as shown in Figure 3b,c. In the case of coexistence of BP, reoxidation of TCNE^{2-} allowed the solution to turn from purple to yellow corresponding to the TCNE$^-$ generation. The solution again showed the 550 nm band

Bistable Charge-Transfer Complex Formation

J. Phys. Chem. A, Vol. 104, No. 13, 2000 **3067**

TABLE 1: Thermodynamic Data of the $\pi-\pi$ CT Complexes in CH_2Cl_2 Containing 0.5 mol dm^{-3} TBAP

complex	formation constants/dm^3 mol^{-1}				$\Delta H°$/kJ mol^{-1}	$\Delta S°$/J mol^{-1} K^{-1}
	288.0 K	293.0 K	298.0 K^a	303.0 K		
CL-HMB	9.40×10^{-1}	8.30×10^{-1}	7.97×10^{-1}	7.19×10^{-1}	-1.23×10	-4.32×10
CL-AN			9.95×10^{-1} (1.08)			
CL-BP	7.45×10^{-1}	6.90×10^{-1}	6.56×10^{-1} (1.19)	6.09×10^{-1}	-9.50	-3.54×10
CL^{2-}-BP	4.76×10	4.13×10	3.39×10 (2.14×10^2)	2.45×10	-3.16×10	-7.74×10
TCNE-HMB	4.08	3.69	3.35 (8.79)	2.78	-1.80×10	-5.06×10
TCNE-AN	b	b	b	b		
TCNE-BP	4.89×10^{-1}	4.42×10^{-1}	4.14×10^{-1} (7.56×10^{-1})	4.06×10^{-1}	-9.08	-3.76×10
TCNE^{2-}-BP	3.03×10	2.52×10	2.03×10 (5.82×10)	1.33×10	-3.98×10	-1.03×10^2

^{a} Values in parentheses are observed in CH_2Cl_2 containing 0.1 mol dm^{-3} TBAP. ^{b} Values were not obtained because of formation of an inner complex. See the text for details.
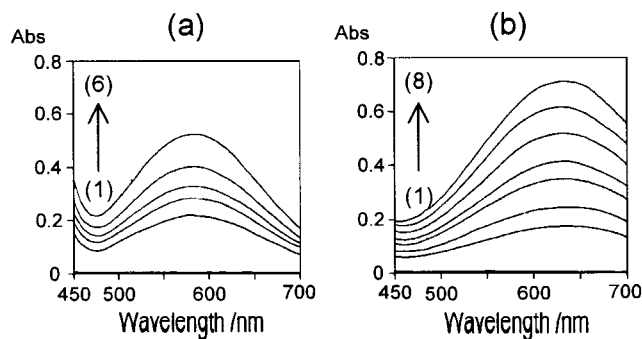

Figure 4. Spectral change of 2.92×10^{-2} mol dm^{-3} BP (a) and 2.50×10^{-2} mol dm^{-3} BP (b) in CH_2Cl_2 containing 0.5 mol dm^{-3} TBAP at 298 K with increasing the concentrations of CL and TCNE, respectively. Concentrations of CL for Figure a (mol dm^{-3}): (1) 0, (2) 8.30×10^{-3}, (3) 1.01×10^{-2}, (4) 1.21×10^{-2}, (5) 1.50×10^{-2}, (6) 2.02×10^{-2}. Concentrations of TCNE for Figure b (mol dm^{-3}): (1) 0, (2) 1.61×10^{-2}, (3) 2.33×10^{-2}, (4) 3.36×10^{-2}, (5) 3.97×10^{-2}, (6) 4.87×10^{-2}, (7) 5.67×10^{-2}, (8) 6.57×10^{-2}. Note here that the spectra of the components show no band in the wavelength region.
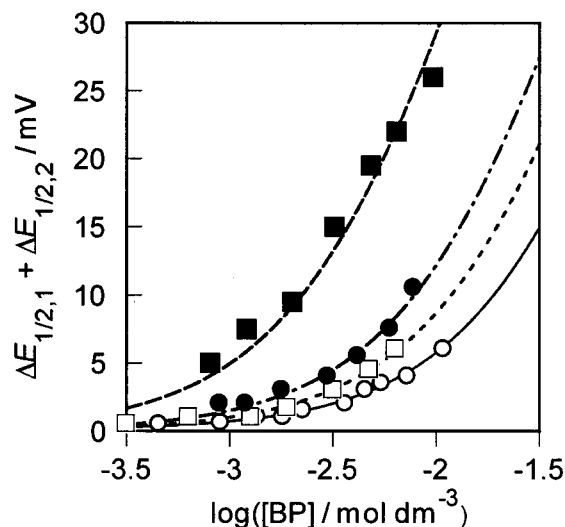

Figure 5. Dependence of ($\Delta E_{1/2,1} + \Delta E_{1/2,2}$) values of CL and TCNE upon the concentrations of BP: (○) TCNE (concentration of TBAP ([TBAP]) = 0.5 mol dm^{-3}); (●) TCNE ([TBAP] = 0.1 mol dm^{-3}); (□) CL ([TBAP] = 0.5 mol dm^{-3}); (■) CL ([TBAP] = 0.1 mol dm^{-3}). Curves represent the regression curves analyzed on the basis of eq 3.

by reduction into TCNE^{2-}. The reversible color change in the TCNE solution with redox reactions indicates that the spectral change corresponds to the redox equilibria involving the CT complex formation of TCNE^{2-} with BP. As far as we know, this is a novel observation of the intermolecular CT spectra of the organic π-dianions.

Thermodynamic Data for the CT Complex Formation of the Neutral and Dianionic Species with BP. To treat the situation more quantitatively, we have estimated the CT complex
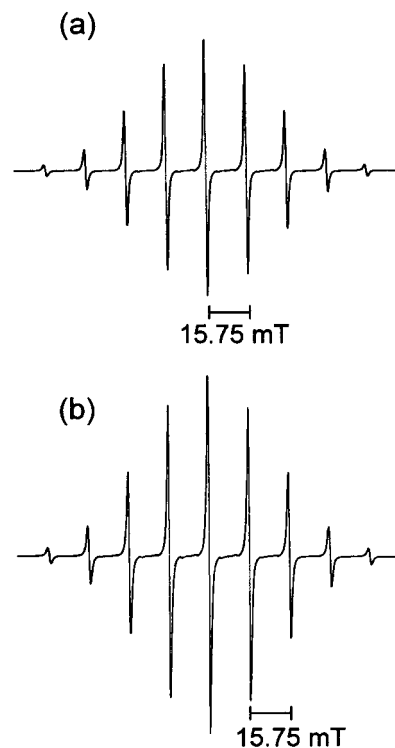

Figure 6. ESR spectra of TCNE$^-$ electrogenerated in CH_2Cl_2 containing 0.5 mol dm^{-3} TBAP in the absence (a) and the presence (b) of 1.01×10^{-2} mol dm^{-3} BP.

formation constants of the neutral, mono-, and dianionic species of CL and TCNE. It is well known that CL and TCNE as strong acceptors form the CT complexes with the hydrocarbons, giving the intermolecular CT spectra in a longer wavelength region than those of the components.[28,29] Figure 4 shows the CT spectra of the CL-BP and TCNE-BP systems. It is clearly found that the absorbance in the newly appeared bands of 585 and 620 nm for the CL-BP and TCNE-BP systems, respectively, increases with increasing the concentrations of the components. The CT spectra were also observed in the other systems containing the hydrocarbons except for the TCNE-AN system. These spectral behaviors allow the complex formation constants (K) to be estimated from the Benesi-Hildebland and Lang equations.[30,31] The excellent linear plots based on the equations were observed, the estimated K values being summarized in Table 1.

To quantify the binding of the anion radicals and the π-dianions with BP, we noted the dependence of the first and second half-wave reduction potentials upon concentrations of BP ([BP]). The dependence of reduction potentials on the concentrations of additives has been analyzed for the systems involving the reaction interpreted in terms of the association equilibria of the redox species with the additives such as hydrogen bonding and inclusion interaction.[10,32] By analogy with
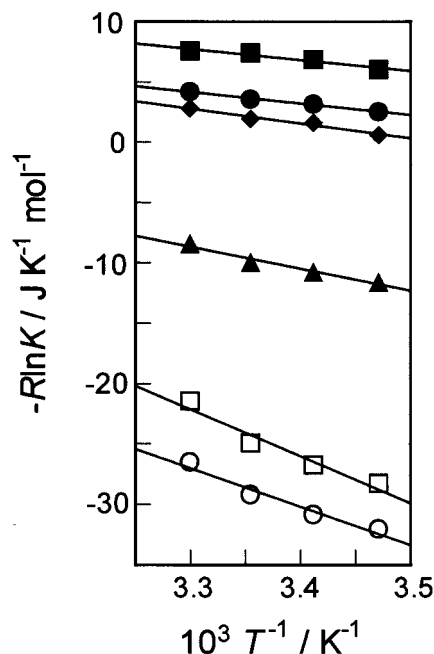
Figure 7. Linear relations of -RlnK values to T^{-1} values for various CT complexes: (●) TCNE-BP; (■) CL-BP; (▲) TCNE-HMB; (◆) CL-HMB; (○) TCNE^{2-}-BP;. (□) CL^{2-}-BP.

the treatment, we write the potential shift for the first and second reduction steps ($\Delta E_{1/2,1}$ and $\Delta E_{1/2,2}$, respectively) as follows, based on the assumption that the diffusion coefficients are equal through the redox species and their CT complexes, and the bulk concentration of BP is much larger than that of CL or TCNE:

$$\Delta E_{1/2,1} = -\frac{RT}{F}\ln\frac{(1 + K[BP])}{(1 + K^-[BP])} \tag{1}$$

$$\Delta E_{1/2,2} = -\frac{RT}{F}\ln\frac{(1 + K^-[BP])}{(1 + K^{2-}[BP])} \tag{2}$$

where $\Delta E_{1/2}$ is defined as $E_{app,1/2} - E_{1/2}$, $E_{1/2}$ and $E_{app,1/2}$ being the half-wave reduction potentials, taken as the midpoint between the cathodic and anodic peak potentials in the cyclic voltammograms, in the absence and the presence of BP, respectively, and K^- and K^{2-} denote the CT complex formation constants of the mono- and dianionic species with BP, respectively. The sum of eqs 1 and 2 leads to

$$\Delta E_{1/2,1} + \Delta E_{1/2,2} = -\frac{RT}{F}\ln\frac{(1 + K[BP])}{(1 + K^{2-}[BP])} \tag{3}$$

Nonlinear regression analyses based on eq 3 allow values of K^{2-} to be estimated using the K values given in Table 1. Typical examples of the nonlinear plots based on eq 3 are given in Figure 5. The values of K^{2-} are collected in Table 1. The formation of the CT complexes is significantly affected by concentrations of coexisting electrolytes. An increase in the concentrations of electrolytes decreases the CT complex formation ability of the dianions as well as the neutral species, as shown in Table 1 and Figure 5. This behavior for the neutral CT complexes is well documented in the published works.[28,29]

Although errors in measurement of the small changes in $E_{1/2,1}$ led to considerable uncertainty in the values of K^-, the K^- values were estimated by nonlinear regression analyses based on eq 1 as about 0. Figure 6 shows the ESR spectra of TCNE$^-$ in the absence and the presence of BP. The spectra and the coupling
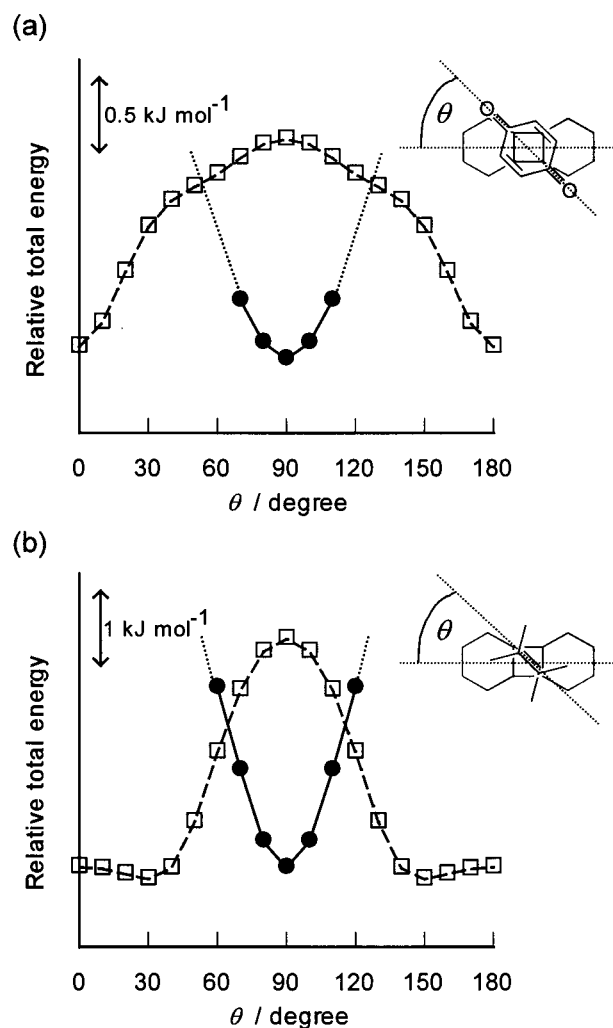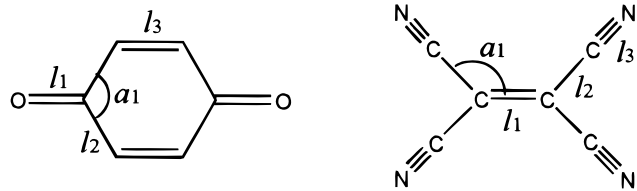

Figure 8. Dependence of the relative HF/6-31G(d) total energies of the CL^{n-}−BP (a) and TCNE^{n-}−BP (b) complexes upon θ. The filled circles correspond to the dianions ($n = 2$) and the open squares to the neutral species ($n = 0$). The definition of θ is shown in the figures.

constant of the nitrogen atom were in excellent agreement with those previously published.[33] It is evidently shown that the ESR spectra are not quite influenced by the presence of BP. This implies that the BP does not interact with TCNE$^-$ in terms of at least the CT interaction. In addition, the color of the TCNE$^-$ solution remains yellow in the presence of BP. This situation led to the conclusion that the anion radical does not form the CT complexes with BP.

Temperature dependence of the K and K^{2-} values yields the formation energy from the slope of the linear relation between $-R\ln K$ (or $-R\ln K^{2-}$) values and T^{-1} values. Figure 7 shows the good linear relations of the present systems, $\Delta H°$ and $\Delta S°$ values being collected in Table 1. The results show that the CT complex formation of the dianions as well as the neutral species is considered as enthalpy-driven stabilization.[28,29]

Geometries of CL^{2-}, TCNE^{2-} and Their CT Complexes. The structure of the 1,4-benzoquinone dianion has been characterized by the formal single C═O bonds and the aromatic ring.[9-11] The structure of CL^{2-} is similar to it, as is seen from Table 2. On the other hand the structural properties of TCNE^{2-} have been investigated in a previous paper[27] by spectral measurements and MO calculations at SCF, MP2, and MP4 levels with 6-31G(d), 6-31+G(d), and 6-311+G(d) basis sets on the rotational barrier around the formal single C═C bond of TCNE^{2-}. It has been concluded that TCNE^{2-} preferentially

Bistable Charge-Transfer Complex Formation

J. Phys. Chem. A, Vol. 104, No. 13, 2000 **3069**

TABLE 2: Optimized Bond Distances and Angles, and Energies of Free and Complexed CL, CL^{2-}, TCNE, TCNE^{2-} and BP by HF/6-31G(d) Calculations

	bond distance (angle)/Å (°)							energy/kJ mol^{-1}	
	l_1	l_2	l_3	a	l_4	l_5	l_6	SCF	MP2
BP					1.5073	1.4136	1.3569	−1205142.796	−1209104.993
CL	1.1822	1.5014	1.3255	117.38				−5814957.322	−5819237.135
CL^{2-}	1.2587	1.4229	1.3922	110.37				−5814809.654	−5819195.973
CL−BP	1.1819	1.5013	1.3251	117.23	1.5076	1.4144	1.3574	−7020109.442	−7028377.996
CL^{2-}−BP	1.2592	1.4229	1.3923	110.40	1.5058	1.4124	1.3561	−7019940.797	−7028306.646
TCNE	1.3368	1.4407	1.1340	121.84				−1168133.598	−1171698.304
TCNE^{2-} ^{a}	1.5196	1.3964	1.156	122.15				−1168049.806	−1171642.982
TCNE−BP	1.3366	1.4410	1.1339	121.79	1.5080	1.4146	1.3575	−2373290.954	−2380838.654
TCNE^{2-}−BP	1.5184	1.3971	1.1562	122.33	1.5052	1.4128	1.3971	−2373182.061	−2380767.024

^{a} Calculated for the D_{2h} structure. See the text for details.

adopts the planar D_{2h} structure in CH$_2$Cl$_2$.[27] The D_{2h} structure is thus taken into consideration in the present work.[34] The significant change in the D_{2h} structure with two-electron addition to the LUMO is a lengthening of the C=C bond, as shown in Table 2. Figure 8 shows dependence of the HF/6-31G(d) energies upon the stacking angle (θ) of the components in the CL−BP and TCNE−BP systems, indicating that the orientation of the components in the dianion systems is different from that in the neutral systems. The formation of the most stable CL^{2-}−BP and TCNE^{2-}−BP complexes is observed at $\theta = 90°$, whereas the geometries of $\theta = 0°$ give the most stable complexes for the neutral species. In the case of the dianion complexes at θ values less than 50° and more than 130°, the stacking distances were optimized in length without any interaction. The optimized geometries are illustrated in Figure 9 and are listed in Table 2. The stacking distances for the TCNE and TCNE^{2-} complexes are suitable for the favorable $\pi-\pi$ intermolecular interaction.[28] The CL^{2-}−BP complex was optimized at a somewhat long distance. This seems to be ascribed to an overestimate of the steric repulsion between BP and the chlorine atoms fixed on the quinoide plane of CL. The full optimization was, however, not possible because of computer cost. No major changes are brought about on the internal geometries of the components as a result of the CT complex formation, as shown in Table 2. This is a general property of the $\pi-\pi$ type CT complexes based on the face-to-face interaction between two delocalized π-electronic systems without point-to-point interaction such as hydrogen bonds.[28,29]

In addition, the present calculations provided information on the formation energies and the direction of CT in the complexes. The formation energies were predicted at the MP2 level as 5.7 (CL^{2-}−BP) and 19.0 kJ mol^{-1} (TCNE^{2-}−BP) from the data listed in Table 2.[35,36] The magnitude of CT was calculated as −0.002 and −0.020 for the CL^{2-}−BP and TCNE^{2-}−BP systems, respectively.[35,37] The results thus indicate that the dianions form the stable CT complexes with BP, as electron donors. The underestimate for the CL^{2-}−BP system is again due to the poor modeling.

Theory on the Intermolecular CT Complex Formation of the π-Dianions. Next, discussion was extended to the characteristic molecular recognition of the dianions for BP, giving clear-cut evidence for the geometrical configuration of the dianion complexes. Figure 10 shows the energy levels and
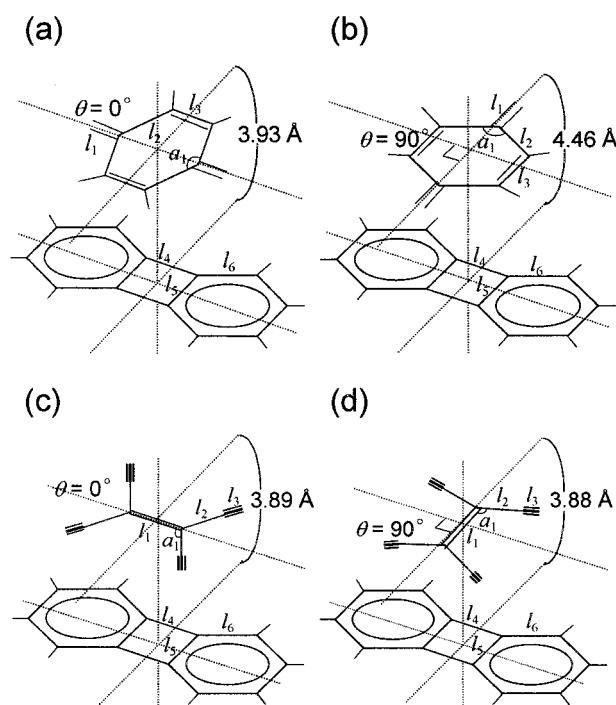

Figure 9. Optimized geometries of the CL (a), CL^{2-} (b), TCNE (c), and TCNE^{2-} (d) complexes with BP obtained by HF/6-31G(d) calculations. Values of bond distance and angles are listed in Table 2.

illustrations of MOs with regard to the CT interaction. The MO characters of HMB were the same as those of AN except for degeneration in the HOMO and the LUMO. Mulliken's CT theory indicates that formation of the $\pi-\pi$ CT complexes requires the maximum overlap and small energy gap of the HOMO of donors and the LUMO of acceptors.[28] The b_{2g}-LUMO of CL favorably interacts with the b_{2g}-HOMO of BP at $\theta = 0°$ and the b_{3g}-HOMO of AN at $\theta = 90°$, as shown in Figure 10a.[38] This is particularly related to the former factor of Mulliken's theory. Similarly, the TCNE−BP and TCNE−AN complexes are reasonably explained by the favorable HOMO−LUMO interaction (Figure 10c). The intermolecular interaction of the b_{3g}-HOMO of CL^{2-} (donor) and the b_{3g}-LUMO of BP (acceptor) favors the CT complex formation at $\theta = 90°$ in terms of the bonding character of the MO phases, whereas the HOMO−
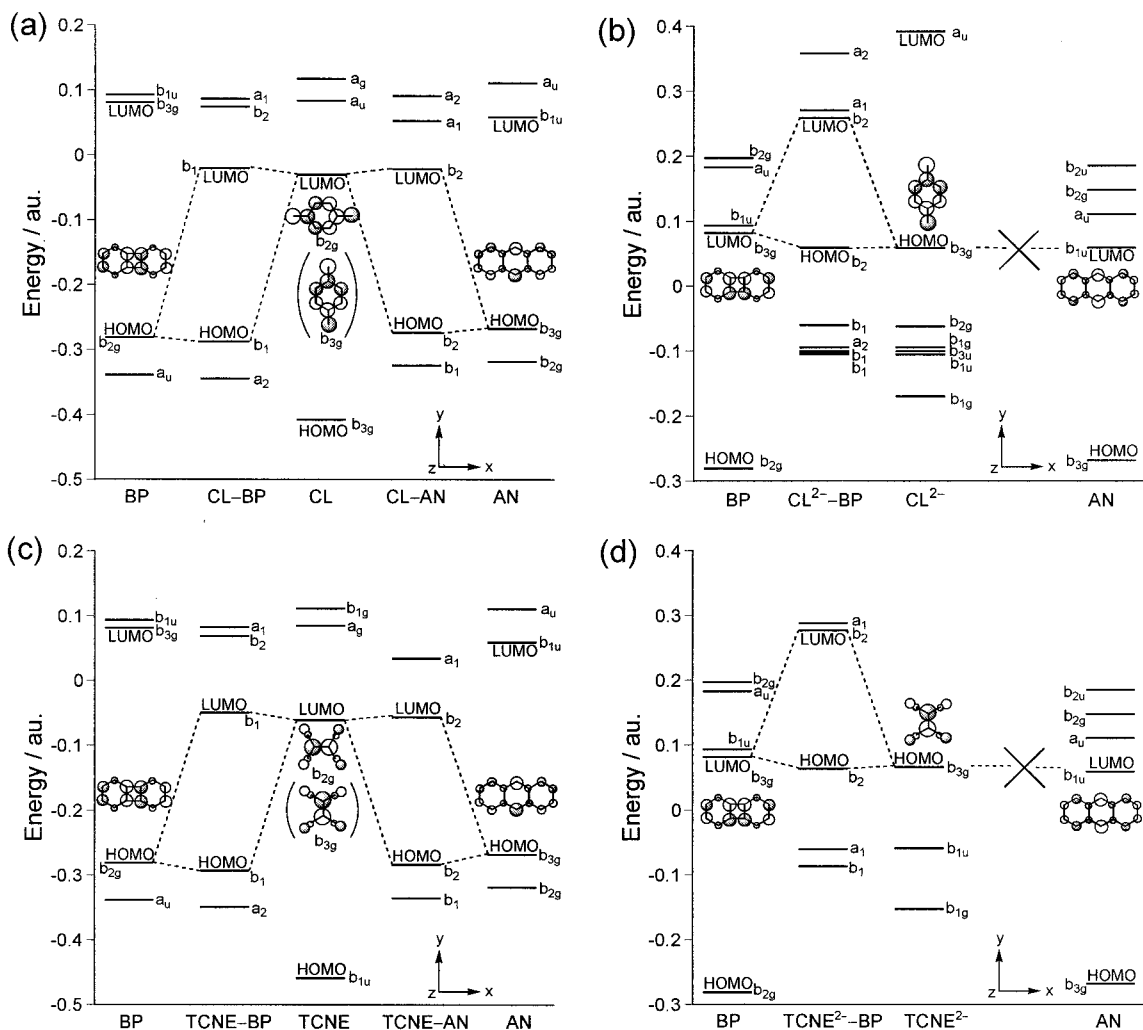
Figure 10. RHF/6-31G(d) MO energy levels and the MO illustrations concerning the CT complex formation of CL (a), CL^{2-} (b), TCNE (c), and $TCNE^{2-}$ (d) with the hydrocarbons. 1au. = 2625.500 kJ mol^{-1}.

LUMO interaction of CL^{2-} and AN is unfavorable at any values of θ (Figures 10b). Figure 10d displays the same situation for the $TCNE^{2-}$ complex formation. The orbital character appeared in BP seems to be a property of the $4n\pi$ electronic systems under D_{2h} symmetry in consideration of the number of electrons and constitution of the MOs. The HOMO−LUMO energy gap (the later factor of Mulliken's theory) is an important, necessary, but not sufficient factor to form the CT complexes. Indeed, CL^{2-} does not form the CT complex with AN whose electron affinity is larger than that of BP,[39] as mentioned in the previous section. These results reasonably indicate that the molecular recognition of the dianions forming the CT complexes is primarily governed by the orbital symmetry, which plays a crucial role in determining the geometry of the CT complexes.

Molecular Recognition in the Redox-Mediated Bistable Complex Formations. The experimental and theoretical results given here enable us to generate the redox-mediated bistable complex systems, as shown in Figure 11. We have great interest in sufficiently different optical spectra and geometries that allow the individual states to be addressed. The trichromic change is ascribed to the chromatic bistable complex formation upon redox state change controlled electrochemically; blue, orange, and red in the CL−BP system and green-blue, yellow, and purple in the TCNE−BP system, resulting from the neutral complex formation, the anion radical generation and the complex formation of the dianions, respectively, as shown in Figure 11. Indeed, the bistable complex formation is apparently confirmed

by the reversible color change of the bulk electrolysis solutions with change in applied potentials. The bistable complex formation is based on the interconversion of the intermolecular HOMO−LUMO interaction modulated by the redox reactions. This is particularly related to the geometrical alteration in the systems because the π−π interaction occurs at multipoints of the π-electronic systems. The π−π CT complexes as well as hydrogen bonds will play an important role in engineering highly designed, redox-mediated molecular recognition systems by virtue of their colors and geometries.

Conclusions

It has been demonstrated that the organic π-dianions form the π−π type CT complexes characterized by the geometry, and the spectrum is different from those of the neutral complexes. This is a novel observation of the intermolecular CT interaction of the dianions. The bistable systems proposed here are primarily based on intermolecular recognition which characteristically occurs in the dianions forming the CT complex with the $4n\pi$ electronic system of BP, and interconversion of the intermolecular HOMO−LUMO interaction modulated by a redox event. This is also an original approach to the redox-mediated bistable complex formation. To extend this approach to a specific recognition system, it is desirable to probe the recognition elements having the larger formation constants. This can be achieved by discussion on the intermolecular HOMO−
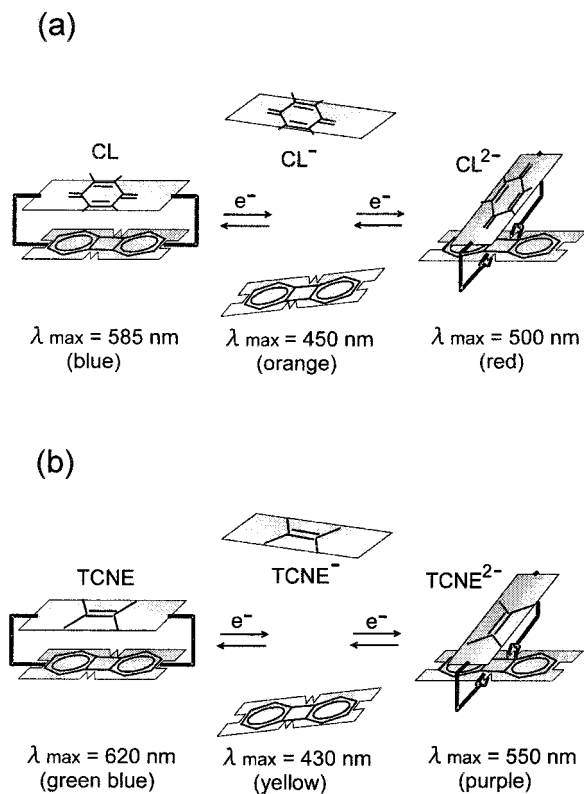
Bistable Charge-Transfer Complex Formation

J. Phys. Chem. A, Vol. 104, No. 13, 2000 **3071**

(a)

CL

CL⁻

CL²⁻

e^- e^-

λ_{max} = 585 nm
(blue)

λ_{max} = 450 nm
(orange)

λ_{max} = 500 nm
(red)

(b)

TCNE

TCNE⁻

TCNE²⁻

e^- e^-

λ_{max} = 620 nm
(green blue)

λ_{max} = 430 nm
(yellow)

λ_{max} = 550 nm
(purple)

Figure 11. Redox-mediated bistable complex formation with the geometrical alteration and the trichromic change in the TCNE−BP (a) and CL−BP systems (b).

LUMO energy gap between the components in future work. The present conclusion is important for extended discussion on generation of the highly designed, redox-mediated recognition systems involving the electrogenerated π-dianions and the design of molecular devices utilizing the recognition.

References and Notes

(1) (a) Lehn, J.-M. *Supramolecular Chemistry. Concepts and Perspectives*; VCH: Weiheim, 1995. (b) Beer, P. D. *Acc. Chem. Res.* **1998**, *31*, 71.

(2) Kaifer, E. A. *Acc. Chem. Res.* **1999**, *32*, 62, and references therein.

(3) Niemz, A.; Rotello, V. M. *Acc. Chem. Res.* **1999**, *32*, 44, and references therein.

(4) (a) Zahn, S.; Canary, J. W. *Angew. Chem., Int. Ed. Engl.* **1998**, *37*, 305. (b) Beer, P. D.; Szemes, F.; Balzani, V.; Sala, C. M.; Drew, M. G. B.; Dent, S. W.; Maestri, M. *J. Am. Chem. Soc.* **1997**, *119*, 11864. (c) Zelikovich, L.; Libman, J.; Shanzer, A. *Nature* **1995**, *374*, 790. (d) Wytko, J. A.; Boudon, C.; Weiss, J.; Gross, M. *Inorg. Chem.* **1996**, *35*, 4469. (e) Livoreil, A.; Dietrich-Buchecker, C. O.; Sauvage, J.-P. *J. Am. Chem. Soc.* **1994**, *116*, 9399. (f) Kawai, S. H.; Gilet, S. L.; Ponsiner, R.; Lehn, J. M. *Chem. Eur. J.* **1995**, *1*, 285.

(5) (a) Chen, Z.; Pilgrim, A. J.; Beer, P. D. *J. Electroanal. Chem.* **1998**, *444*, 209. (b) Nielson, R. M.; Lyon, L. A.; Hupp, J. T. *Inorg. Chem.* **1996**, *35*, 970.

(6) (a) Francis, D. S. *J. Am. Chem. Soc.* **1996**, *118*, 923. (b) Hayashi, T.; Miyahara, T.; Hashizume, N.; Ogoshi, H. *J. Am. Chem. Soc.* **1993**, *115*, 2049.

(7) (a) Ebata, K.; Setaka, W.; Inoue, T.; Kabuto, C.; Kira, M.; Sakurai, H. *J. Am. Chem. Soc.* **1998**, *120*, 1335. (b) Minskey, A.; Meyer, A. Y.; Poupko, R.; Rabinovitz, M. *J. Am. Chem. Soc.* **1983**, *105*, 2164. (c) Iyoda, M.; Sasaki, S.; Sultana, F.; Yoshida, M.; Kuwatani, Y.; Nagase, S. *Tetrahedron Lett.* **1997**, *37*, 7987.

(8) Bausch, J. W.; Gregory, P. S.; Olah, G. A.; Prakach, G. K. S.; Schleyer, P. v. R.; Segal, G. A. *J. Am. Chem. Soc.* **1989**, *111*, 3633.

(9) Okumura, N.; Uno, B. *Bull. Chem. Soc. Jpn.* **1999**, *72*, 1213.

(10) Uno, B.; Kawabata, A.; Kano, K. *Chem. Lett.* **1992**, 1017.

(11) Zhao, X.; Imahori, H.; Zhan, C. G.; Sakata, Y.; Iwata, S.; Kitagawa, T. *J. Phys. Chem. A* **1997**, *101*, 622.

(12) (a) Oyama, M.; Takei, A.; Okazaki, S. *J. Chem. Soc., Chem. Commun.* **1995**, 1909. (b) Modler-Spreitzer, A.; Mannschreck, A.; Scholz, M.; Gescheidt, G.; Spreitzer, H.; Daub, J. *J. Chem. Res. (S)* **1995**, 180.

(13) (a) Dixon, D. A.; Miller, J. S. *J. Am. Chem. Soc.* **1987**, *109*, 3656. (b) James, R.; Foxman, B. M.; Guarrera, D.; Miller, J. S.; Calabrese, J. C.; Reis, A. H., Jr. *J. Mater. Chem.* **1996**, *6*, 1627.

(14) (a) Wakahara, T.; Kodama, R.; Akasaka, T.; Ando, W. *Bull. Chem. Soc. Jpn.* **1997**, *70*, 665. (b) Stevenson, C. D.; Fico, R. M., Jr. *J. Org. Chem.* **1995**, *60*, 5452.

(15) Gupta, N.; Linschitz, H. *J. Am. Chem. Soc.* **1997**, *119*, 6384.

(16) (a) Aquino, M. A. S.; White, C. A.; Bensimon, C.; Greedan, J. E.; Crutchley, R. J. *Can. J. Chem.* **1996**, *74*, 2201. (b) Kurihara, M.; Saito, I.; Matsuda, Y. *Chem. Lett.* **1996**, 1109. (c) Sekiguchi, A.; Matsuo, T.; Ebata, K.; Sakurai, H. *Chem. Lett.* **1996**, 1133.

(17) Kubota, T.; Kano, K.; Uno, B.; Konse, T. *Bull. Chem. Soc. Jpn.* **1987**, *60*, 3865.

(18) (a) Kubota, T.; Uno, B.; Kano, K.; Ninomiya, Y. *Mol. Cryst. Liq. Cryst.* **1985**, *126*, 111. (b) Uno, B.; Ninomiya, Y.; Kano, K.; Kubota, T. *Spectrochim. Acta A* **1987**, *43*, 935. (c) Uno, B.; Kano, K.; Kaida, N.; Kubota, T. *Spectrochim. Acta A* **1989**, *45*, 937.

(19) Kano, K.; Mori, K.; Konse, T.; Uno, B.; Kutoba, T. *Anal. Sci.* **1989**, *5*, 651.

(20) (a) Frisch, M. J.; Trucks, G. W.; Schlegel, H. B.; Scuseria, G. E.; Robb, M. A.; Cheeseman, J. R.; Zakrzewski, V. G.; Montgomery, J. A.; Stratmann, R. E. Jr.; Burant, J. C.; Dapprich, S.; Millam, J. M.; Daniels, A. D.; Kudin, K. N.; Strain, M. C.; Farkas, O.; Tomasi, J.; Barone, V.; Cossi, M.; Cammi, R.; Mennucci, B.; Pomelli, C.; Adamo, C.; Clifford, S.; Ochterski, J.; Petersson, G. A.; Ayala, P. Y.; Cui, Q.; Morokuma, K.; Malick, D. K.; Rabuck, A. D.; Raghavachari, K.; Foresman, J. B.; Cioslowski, J.; Ortiz, J. V.; Baboul, A. G.; Stefanov, B. B.; Liu, G.; Liashenko, A.; Piskorz, P.; Komaromi, I.; Gomperts, R.; Martin, R. L.; Fox, D. J.; Keith, T.; Al-Laham, M. A.; Peng, C. Y.; Nanayakkara, A.; Gonzalez, C.; Challacombe, M.; Gill, P. M. W.; Johnson, B.; Chen, W.; Wong, M. W.; Andres, J. L.; Gonzalez, C.; Head-Gordon, M.; Replogle, E. S.; Pople, J. A. *Gaussian 98* Gaussian, Inc.: Pittsburgh, 1998. (b) Foresman, J. B.; Frisch, Æ. *Exploring Chemistry with Electronic Structure Methods*, 2nd ed.; Gaussian, Inc.: Pittsburgh, 1993.

(21) The negative shift of the first wave on addition of the hydrocarbons is due to the CT complex formation of neutral CL with the hydrocarbons, see: Peover, M. E. In *Electroanalytical Chemistry*; Bard, A. J. Ed.; Marcel Dekker: New York, 1967; Vol. 2, pp 1−48.

(22) (a) Galus, G. *Fundamentals of Electrochemical Analysis*; Ellis Harwood: Chichester, 1976; Chapter 14. (b) Chauhan, B. G.; Fawcett, W. R.; Lasia, A. A. *J. Phys. Chem.* **1977**, *81*, 1476. (c) Fawcett, W. R.; Opallo, M.; Fedurco, M.; Lee, J. W. *J. Am. Chem. Soc.* **1993**, *115*, 196. (d) Peover, M. E. *J. Chem. Soc.* **1962**, 4540.

(23) Ge, Y.; Lilienthal, R. R.; Smith, D. K. *J. Am. Chem. Soc.* **1996**, *118*, 3976.

(24) (a) Caffrey, M. S.; Daldal, F.; Holden, H. M.; Cusanovich, M. A. *Biochemistry* **1991**, *30*, 4119. (b) Goodin, D. B.; McRee, D. E. *Biochemistry* **1993**, *32*, 3313. (c) Huang, J.; Ostrander, R. L.; Rheingold, A. L.; Walters, M. A. *Inorg. Chem.* **1995**, *34*, 1090.

(25) The spectrum of BP shows two bands at 249 nm (molecular extinction coefficient (ϵ) = 61,400) and 358 nm (ϵ = 8,020) in CH_2Cl_2.

(26) (a) Ueda, H.; Sakabe, N.; Tanaka, J.; Furusaki, A. *Nature* **1967**, *215*, 956. (b) Destro, R.; Gramaccioli, C. M.; Scinonneta, M. *Nature* **1967**, *215*, 389.

(27) Uno, B.; Okumura, N. *Chem. Lett.* **1999**, 1167.

(28) Mulliken, R. S.; Person, W. B. *Molecular Complexes*; Wiley-Interscience: New York, 1969.

(29) Mataga, N.; Kubota, T. *Molecular Interactions and Electronic Spectra*; Marcel Dekker: New York, 1970.

(30) (a) Benesi, H. A.; Hildebrand, J. H. *J. Am. Chem. Soc.* **1949**, *71*, 2703. (b) Lang, R. P. *J. Am. Chem. Soc.* **1962**, *84*, 1185.

(31) The Benesi-Hildebrand equation was used for the systems containing HMB and AN. The Lang equation was applied to the CL−BP and TCNE−BP to overcome the low solubility of BP in CH_2Cl_2. For the latter, a final set of the molecular extinction coefficient (ϵ_{CT}) of the CT band and the K value was obtained from the repeated calculations under convergence on the ϵ_{CT} value of 0.001.

(32) (a) Kano, K.; Mori, K.; Uno, B.; Goto, M.; Kubota, T. *J. Am. Chem. Soc.* **1990**, *112*, 8645. (b) Kano, K.; Mori, K.; Uno, B.; Kutota, T. *J. Electroanal. Chem.* **1990**, *283*, 187.

(33) Rieger, P. H.; Bernal, I.; Reinmuth, W. H.; Fraenkel, G. K. *J. Am. Chem. Soc.* **1963**, *85*, 683.

(34) $TCNE^{2-}$ of the D_{2d} structure is not expected to form the $\pi-\pi$ complex with BP. Indeed, the CT spectrum and the positive shift of the second wave in the voltammogram of TCNE on addition of BP were not observed in CH_3CN in which $TCNE^{2-}$ preferentially adopts the D_{2d} structure.[27]

(35) Nishimoto, K. In *Biomolecules Electronic Aspects*; Nagata, C.; Hatano, M.; Tanaka, J.; Suzuki, H., Eds.; Japan Sci. Soc. Press: Tokyo, Elsevier: Amsterdam, 1985; pp 9−19.

(36) The CT complex formation energy (ΔE) was calculated by the equation: $\Delta E = E(A) + E(BP) - E(A-BP \text{ complex})$, where E denotes the total energy of the molecule shown in parentheses (A = CL, CL^{2-}, TCNE, $TCNE^{2-}$).[35] Calculated ΔE (kJ mol^{-1}): 35.9 (CL−BP complex); 35.4 (TCNE−BP complex).

(37) The magnitude of charge transfer was expressed by charge migration ΔQ: $\Delta Q = Q(BP, \text{complexed}) - Q(BP, \text{free})$ where Q is the sum of gross population of all atoms in the molecule shown in parentheses.[35] The ΔQ values were calculated by the HF/6-31G(d) method as 0.0097 and −0.0020 for the CL−BP and CL^{2-}−BP systems, respectively, and as 0.0096 and −0.0200 for the TCNE−BP and $TCNE^{2-}$−BP systems, respectively.

(38) The b_{2g} symmetry is the same as b_{3g} under the point group D_{2h} on rotation of 90° with regard to the C_2 axis (z) in Figure 10. Thus, the interaction between the b_{3g}-HOMO and the b_{2g}-LUMO is explained by the favorable HOMO−LUMO interaction having the same symmetry.

(39) The half-wave reduction potentials of BP and AN are −2.27 and −1.99 V vs SCE, respectively. The electrochemical behavior of AN is published in a previous paper.[17]